Energy Storage Planning in Active Distribution Grids: A Chance-Constrained Optimization with Non-Parametric Probability Functions

Hossein Akhavan-Hejazi, *Student Member, IEEE*, and Hamed Mohsenian-Rad, *Senior Member, IEEE*

***Abstract*— By considering the specific characteristics of random variables in active distribution grids, such as their statistical dependencies and often irregularly-shaped probability distributions, we propose a non-parametric chance-constrained optimization approach to operate and plan energy storage units in power distribution girds. In particular, we develop new closed-form stochastic models for the key operational parameters in the system. Our approach is analytical and allows formulating tractable optimization problems. Yet, it does not involve any restricting assumption on the distribution of random parameters, hence, it results in accurate modeling of uncertainties. Different case studies are presented to compare the proposed approach with the conventional deterministic and parametric stochastic approaches, where the latter is based on approximating random variables with Gaussian probability distributions.**

***Keywords*: Energy storage, distribution grid, non-parametric probability distributions, chance-constrained optimization, probabilistic optimal power flow, linearized branch model.**

NOMENCLATURE

$\mathcal{N}, \mathcal{L}$	Set of all buses, and all distribution lines.
$\mathcal{N}_i$,$\mathcal{D}_i$	Set of descendants and direct descendants of bus i.
$\mathcal{L}_{i,0}$	Set of lines on the path from bus i to bus 0.
s	Superscript indicating storage.
e	Superscript indicating charging station.
r	Superscript indicating renewable generator.
b	Superscript indicating baseload.
u	Superscript indicating solar panel.
i, j, k, l	Subscripts indicating bus numbers.
(i, j)	Distribution line connecting buses i and j.
P, Q	Functions for active power, and reactive power.
v, V	Functions for voltage, and square of voltage .
v, p, q	Values for square voltage, active, and reactive power.
U, H	Active, and reactive power output of a solar panel.
ϕ	Random part of an operational parameter.
ψ	Decision variable part of an operational parameter.
$[t], \Delta t$	Index of time slot, duration of a time slot.
R, X	Line resistance and reactance.
f, g	Probability density function.
F, G	Cumulative probability distribution function.
κ	Reactive to active power ratio for an energy resource.
λ	Number of solar panels.
ζ	Scale of a random input at power flow distributions.
γ	Scale of a random input at voltage distributions.
$\circledast_{i=1}^{N}$	Convolution integral over N functions.
ϵ	Probability target for a chance constraint.
h	Battery storage efficiency function.
h_{apx}	Battery storage Approximated efficiency function.
η_0	Efficiency coefficient of energy storage system.
Ah	Installed capacity of energy storage system in a bus.
N_{ESS}	Number of total installed energy storage systems.
K_{cp}	Scale factor for capacity to available energy.
π	Scale factor for installation or operation costs.
$\overline{(\cdot)}, \underline{(\cdot)}$	Indicators of maxima and minima of variables.

The authors are with the Department of Electrical and Computer Engineering, University of California, Riverside, CA, USA, e-mails: {hossein.akhavan-hejazi, hamed}@ece.ucr.edu. This work is supported in part by NSF grant ECCS 1253516, CEC grant EISG 13-04TE, and RPU grant EIG 14-2853.

I. INTRODUCTION

A. Motivation

Small and medium size Energy Storage Systems (ESS) have diverse applications in power distribution networks. For example, American Electric Power has recently installed a $1MW$ ESS to relieve pressure on a distribution-level transformer [1]. Distribution-level ESS installations can also relieve the fluctuations caused by generation of distributed generators (DGs) and/ or the charging load of electric vehicles (EVs) [2]. Such fluctuations are often more significant compared to typical baseloads [3]. The traditional distribution systems and their control equipment are not designed for compensating the excessive load / generation across their feeders, yet upgrading the existing system for such short periods of deficiency is not economical. In contrast ESS installations as a *multi-functional* resource, can maintain the system safe operation at low cost, if they are deployed and managed effectively.

Modelling uncertainty is different at distribution level versus at transmission level. For example, it might be reasonable to assume statistical independence and/or Gaussian distributions for the generation outputs of wind and/or solar farms that are scattered across a large transmission network [4]. However, these assumptions may not hold in a distribution grid with renewable DGs and EV charging stations that are confined to a relatively small geographical location due to the dependency in solar irradiance in proximate system buses [5] and the non-standard distribution of EV charging loads [6]. Also, the impact of some fluctuating elements may dominate the overall uncertainty in a distribution grid, making the typical use of the *central limit theorem* less practical. Therefore, a more general non-parametric approach (with no restricting assumption on the distribution of random parameters) could be more appropriate for ESS optimization at distribution level.

While non-parametric optimization has been adopted in a verity of problems in power systems, e.g. see [7]–[9], the aim of this paper is to incorporate non-parametric stochastic modelling and optimization in power distribution systems, by addressing the specific characteristics of such systems to optimally operate and plan ESS for improved grid performance.

B. Comparison to Related Literature

With respect to the scope of this paper, the related literature can be classified into several groups. First, some previous studies, e.g., in [10]–[13], are based on the assumption of *complete knowledge* of the hourly generation, demand, etc. Accordingly, despite their different design objectives and methodologies, they can all be classified as *deterministic* methods. In contrast, here, our focus is on stochastic optimization of ESS.

Second, there are studies, e.g., in [14]–[16], that *do* recognize uncertainties in ESS and distribution generation (DG) planning. However, they require fitting Gaussian or other parametric distributions into random variables. Accordingly, their design efficiency can degrade significantly if the Gaussian or other parametric distribution approximations are not accurate.

Third, there are studies, such as in [17]–[21], that address uncertainty *without* restricting the analysis to pre-determined parametric distributions of random variables; however, they account for uncertainties by defining *many instances* of each random variable. For example, the studies in [17], [18] use Monte-Carlo simulation methods. Accordingly, they must deal with a large number of scenarios. Such large-scale scenario generation is tractable if the focus is primarily on analysis, as opposed to on design and optimization. Other studies, e.g. in [19]–[21], utilize stochastic programing to address uncertainties which also involves scenario generation. Such methods are capable to incorporate non-linear but convex power flow equations by solving a deterministic problem over many samples of random variables; yet concerns do exist about the convergence and accuracy of the solution once the number of scenarios increases. In contrast, here in this paper, we take an *analytical* approach where we improve modeling efficiency without exploding the computation workload, but of course with the limitation of linearizing the power flow equations.

Forth, there are studies, e.g. in [22]–[25], that use chance-constrained optimization for optimal operation and planning of resources, mainly in transmission systems. For example, in [22] a chance-constrained optimal power dispatch strategy is developed for transmission systems, using cumulant-based stochastic models. The Gram-Charlier expansion method is applied in [22], [26], [27] to approximate the distribution of state variables; however, it reduces the accuracy of stochastic modelling. Such reduced accuracy could be inevitable in large transmission systems; but it may not be acceptable at distribution level, which is where we focus on in this paper. Also, the DC power flow equations used in [22]–[26] are not appropriate to represent power distribution systems.

Last but not least, our design approach in this paper is also fundamentally different from the fifth group of prior work, e.g., in [28]–[32], where heuristics such as Genetic Algorithms are used to optimize ESS in distribution networks.

C. Technical Contributions

The contributions in this paper are summarized as follows:

- We propose a new non-parametric chance-constrained optimization approach to operate and plan ESS in power distribution networks. Uncertainty from different sources of different stochastic nature, e.g. DGs, EVs, and residential baseloads are taken into consideration.

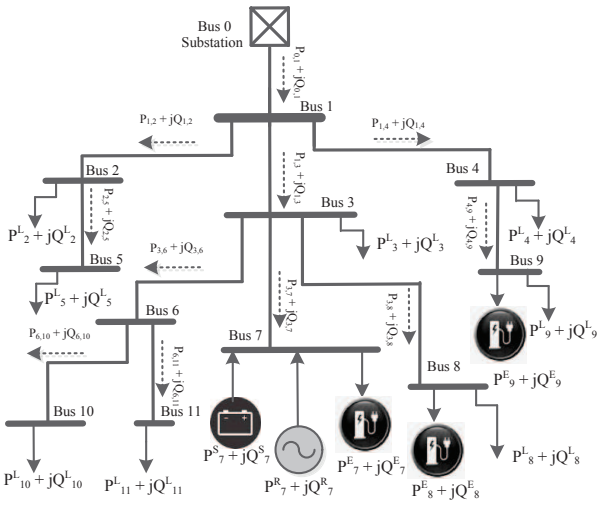

Fig. 1. An example radial distribution network with 12 distribution buses.

- Our analysis is based on developing new closed-form stochastic models for various key operational parameters of the distribution grid. This allowesd us to formulate optimization problems for ESS operation and planning that are in the form of tractable linear programs (LPs) or mixed integer linear programs (MILP). In principle, the developed closed-form stochastic models can be used also in other non-ESS distribution-level planning problems.
- Our ESS planning framework is customized for distribution grids, as opposed to some commonly used models that are based on Gaussian approximations of random variables that were originally intended for transmission systems. For example, our design accounts for the typical radial configuration of the distribution networks as well as the close proximity of distribution buses that causes statistical dependency across certain random variables.
- Several case studies confirmed the advantages of non-parametric chance-constrained optimization over deterministic and parametric chance-constrained optimization.

II. Stochastic System Model

A. Notations and Power Flow Equations

Consider a radial distribution network, such as the one in Fig. 1. Let $\mathcal{N}$ denote the set of all buses, including *reference bus 0*. Also let $\mathcal{L}$ denote the set of all distribution lines. We define $\mathcal{N}^s$, $\mathcal{N}^e$, $\mathcal{N}^r$, and $\mathcal{N}^b$ as the sets of buses with storage units, EV charging stations, renewable DG units, and baseloads, respectively. At each bus i, we define $\mathcal{D}_i$ and $\mathcal{N}_i$ as the sets of direct descendant and descendant buses of bus i, where $\mathcal{D}_i \subseteq \mathcal{N}_i$. We also define $\mathcal{L}_{i,0}$ as the set of lines that connect bus i to bus 0. As an example, in Fig. 1, we have $\mathcal{N}^e = \{7, 8, 9\}$, $\mathcal{N}^r = \mathcal{N}^s = \{7\}$ and $\mathcal{N}^b = \{2, 3, 4, 5, 8, 9, 10, 11\}$. At bus 3, we have $\mathcal{D}_3 = \{6, 7, 8\}$ and $\mathcal{N}_3 = \{6, 7, 8, 10, 11\}$. Set $\mathcal{L}_{7,0} = \{(0, 1), (1, 3), (3, 7)\}$.

Suppose the operation time is divided into T time slots. For each line (i, j), let $P_{(i,j)}[t]$ and $Q_{(i,j)}[t]$ denote the line active and reactive power flows at time slot t. The voltage at bus i at time slot t is denoted by $V_i[t]$. At each bus i, the active

power draw at time slot t is denoted by $P_i^s[t]$, $P_i^e[t]$, $P_i^r[t]$, and $P_i^b[t]$, for storage units, EV charging stations, renewable DG units, and baseloads, respectively. A negative power draw means power injection. The notations $Q_i^s[t]$, $Q_i^e[t]$, $Q_i^r[t]$, and $Q_i^b[t]$ are defined similarly for reactive power.

Next, we model power flows in the distribution grid using the linearized DistFlow equations, which are widely used in the literature, e.g., see [33]–[35]. For all non-reference buses $i \in \mathcal{N}\backslash 0$, and all distribution lines $(i,j) \in \mathcal{L}$ we have:

$$\tilde{P}_{(i,j)}[t] = P_j^s[t] + \tilde{P}_j^b[t] + \tilde{P}_j^e[t] + \tilde{P}_j^r[t] + \sum_{l \in \mathcal{D}_j} \tilde{P}_{(j,l)}[t] \quad (1)$$

$$\tilde{Q}_{(i,j)}[t] = Q_j^s[t] + \tilde{Q}_j^b[t] + \tilde{Q}_j^e[t] + \tilde{Q}_j^r[t] + \sum_{l \in \mathcal{D}_j} \tilde{Q}_{(j,l)}[t] \quad (2)$$

$$\tilde{\mathrm{v}}_i^2[t] - \tilde{\mathrm{v}}_j^2[t] = 2R_{(i,j)}\, \tilde{P}_{(i,j)}[t] + 2X_{(i,j)}\, \tilde{Q}_{(i,j)}[t], \quad (3)$$

where $\mathrm{v}_0 = 1$ and the tilde sign indicates *random* variables. Bus 0 serves as a slack bus with infinite supply capability. Note that, the DistFlow model is originally non-linear and non-convex. Certain convex relaxation techniques are proposed, e.g., in [36], that are exact under certain deterministic formulations. However, those techniques are not applicable in chance-constrained programming. See Section IV-D for additional discussions on the impact of the DistFlow model linearzation.

For the ease of notation, for the rest of this paper we denote:

$$V \triangleq \mathrm{v}^2. \quad (4)$$

Given the above one-to-one relation, we refer to V as voltage, even though it is technically voltage squared. Obtaining all characteristics of v from V is straightforward.

B. Stochastic Representation of Key Operational Parameters

We classify the parameters and variables in a distribution grid into three groups: First, the *key operational parameters*, i.e., the voltages at all buses and the power flows at all lines; second, all *random variables*, i.e., baseloads, EV charging loads, and renewable DG outputs at all buses; third, our *decision variables*, i.e., the charge and discharge powers of all ESS units. Using the recursive relationships in (1)-(3), we can describe the key operational parameters in the first group in terms of the variables in the second and the third groups:

$$\tilde{P}_{(i,j)}[t] = \sum_{k \in \mathcal{N}_j} P_k^s[t] + \sum_{k \in \mathcal{N}_j} \left(\tilde{P}_k^b[t] + \tilde{P}_k^r[t] + \tilde{P}_k^e[t] \right), \quad (5)$$

$$\tilde{Q}_{(i,j)}[t] = \sum_{k \in \mathcal{N}_j} Q_k^s[t] + \sum_{k \in \mathcal{N}_j} \left(\tilde{Q}_k^b[t] + \tilde{Q}_k^r[t] + \tilde{Q}_k^e[t] \right), \quad (6)$$

and

$$\begin{aligned} \tilde{V}_i[t] =& 1 - \sum_{(k,j) \in \mathcal{L}_{i,0}} \left(2R_{(k,j)}\, P_{(k,j)}[t] + 2X_{(k,j)}\, Q_{(k,j)}[t] \right) \\ =& 1 - \sum_{(k,j) \in \mathcal{L}_{i,0}} \sum_{l \in \mathcal{N}_j} \left(2R_{(k,j)}\, P_l^s[t] + 2X_{(k,j)}\, Q_l^s[t] \right) \\ & - \sum_{(k,j) \in \mathcal{L}_{i,0}} \sum_{l \in \mathcal{N}_j} \Big[2R_{(k,j)} \left(\tilde{P}_l^b[t] + \tilde{P}_l^r[t] + \tilde{P}_l^e[t] \right) \\ & + 2X_{(k,j)} \left(\tilde{Q}_l^b[t] + \tilde{Q}_l^r[t] + \tilde{Q}_l^e[t] \right) \Big]. \end{aligned} \quad (7)$$

We can see that each line power flow or each bus voltage is formulated as a sum of a *deterministic* term and a *stochastic* term. The former is a linear combination of ESS injection *decision variables* while the latter is a linear combination of power draw from random variables at different buses.

Given the expressions in (5), (6), and (7), at each time slot t, we can define the Cumulative Distribution Functions (CDFs) for the distribution line active power flows as

$$\begin{aligned} F_{(i,j)}^P[t](p) &\triangleq \Pr\left\{ \tilde{P}_{(i,j)}[t] \le p \right\} \\ &= \Pr\left\{ \tilde{\phi}_{(i,j)}^P[t] \le p - \psi_{(i,j)}^P[t] \right\}, \end{aligned} \quad (8)$$

and for reactive power flows and voltages as

$$F_{(i,j)}^Q[t](q) \triangleq \Pr\left\{ \tilde{\phi}_{(i,j)}^Q[t] \le q - \psi_{(i,j)}^Q[t] \right\}, \quad (9)$$

$$F_i^V[t](v) \triangleq 1 - \Pr\left\{ \tilde{\phi}_i^V[t] \le 1 - v - \psi_i^V[t] \right\}, \quad (10)$$

where

$$\tilde{\phi}_{(i,j)}^P[t] \triangleq \sum_{k \in \mathcal{N}_j} \left(\tilde{P}_k^b[t] + \tilde{P}_k^r[t] + \tilde{P}_k^e[t] \right), \quad (11)$$

$$\tilde{\phi}_{(i,j)}^Q[t] \triangleq \sum_{k \in \mathcal{N}_j} \left(\tilde{Q}_k^b[t] + \tilde{Q}_k^r[t] + \tilde{Q}_k^e[t] \right), \quad (12)$$

$$\tilde{\phi}_i^V[t] \triangleq \sum_{(k,j) \in \mathcal{L}_{i,0}} \left(2R_{(k,j)}\, \tilde{\phi}_{(k,j)}^P[t] + 2X_{(k,j)}\, \tilde{\phi}_{(k,j)}^Q[t] \right), \quad (13)$$

and

$$\psi_{(i,j)}^P[t] \triangleq \sum_{k \in \mathcal{N}_j} P_k^s[t], \qquad \psi_{(i,j)}^Q[t] \triangleq \sum_{k \in \mathcal{N}_j} Q_k^s[t], \quad (14)$$

$$\psi_i^V[t] \triangleq \sum_{(k,j) \in \mathcal{L}_{i,0}} \left(2R_{(k,j)}\, \psi_{(k,j)}^P[t] + 2X_{(k,j)}\, \psi_{(k,j)}^Q[t] \right). \quad (15)$$

Note that, the expressions in (11)-(13) depend solely on random variables and the expressions in (14)-(15) depend solely on the decision variables of the storage units.

At each bus i and time slot t, the Probability Density Function (PDF) for baseload, EV charging load, and renewable generation is denoted by $f_i^b[t](\cdot)$, $f_i^e[t](\cdot)$, and $f_i^r[t](\cdot)$, respectively. These random variables are represented by discrete empirical distributions *with no specific mathematical expressions*. Also, $f_{(i,j)}^P[t](\cdot)$, $f_{(i,j)}^Q[t](\cdot)$, and $f_i^V[t](\cdot)$ denote the PDFs of the system operational parameters at each line and each bus.

Next, we *group* the random variables based on their *statistical dependence*. For example, the outputs of all solar panels are dependent due to their proximity, given the relatively small size of distribution grids. Accordingly, such outputs can be grouped such that they can all be represented in terms of *solar irradiance* as the independent random variable. Other grouping can be done for other renewable DGs of the same type.

Without loss of generality, suppose solar panels are the only DG types on the distribution grid. Let $\tilde{U}[t]$ and $\tilde{H}[t] = \kappa^u[t]\, \tilde{U}[t]$ denote the active and reactive power outputs of a solar panel at time slot t, where κ^u is a constant of the solar panel and its power electronics interface [37]. The PDF of the random variable $\tilde{U}[t]$, i.e. *a unit of solar panel active power output*, is expressed by $f^u[t](\cdot)$. At each bus $i \in \mathcal{N}^r$, we have:

$$\tilde{P}_i^r[t] = \lambda_i^u\, \tilde{U}[t], \quad \tilde{Q}_i^r[t] = \lambda_i^u\, \kappa^u[t]\, \tilde{U}[t], \quad (16)$$

where λ_i^U is a constant that is set for the the DG installation at bus i. Random variable $\tilde{U}[t]$ solely depends on solar irradiance. *Statistical dependency* also exists among active and reactive power injections at each bus [38]. Therefore, at each bus i, we assume that $\tilde{Q}_i^b[t] = \kappa_i^b[t]\tilde{P}_i^b[t]$ and $\tilde{Q}_i^e[t] = \kappa_i^e[t]\tilde{P}_i^e[t]$, where κ_i^b depends on the type of loads and their power electronics interfaces and κ_i^e depends on the EV chargers.

Theorem 1: The CDFs in (8)-(10) are obtained as

$$F^P_{(i,j)}[t](p) = G^{\phi^P}_{(i,j)}[t]\Big(p - \psi^P_{(i,j)}[t]\Big), \tag{17}$$

$$F^Q_{(i,j)}[t](q) = G^{\phi^Q}_{(i,j)}[t]\Big(q - \psi^Q_{(i,j)}[t]\Big), \tag{18}$$

$$F^V_i[t](v) = 1 - G^{\phi^V}_i[t]\Big(1 - v - \psi^V_i[t]\Big), \tag{19}$$

where G^{ϕ^P}, G^{ϕ^Q}, and G^{ϕ^V} are some CDFs that have the following probability density functions:

$$g^{\phi^P}_{(i,j)}[t](z) \triangleq \zeta^u_{(i,j)}\Bigg(\mathop{\circledast}_{k\in\mathcal{N}_j} f^b_k[t] * f^e_k[t](z)\Bigg) * f^u[t]\big(\zeta^u_{(i,j)}z\big), \tag{20}$$

$$\begin{aligned} g^{\phi^Q}_{(i,j)}[t](z) \triangleq{}& \frac{\zeta^u_{(i,j)}\prod_{k\in\mathcal{N}_j}\big(\kappa^b_k[t]\kappa^e_k[t]\big)}{\kappa^u[t]} f^u[t]\big(\frac{\zeta^u_{(i,j)}z}{\kappa^u[t]}\big) \\ &* \Bigg(\mathop{\circledast}_{k\in\mathcal{N}_j} f^b_k[t]\big(\frac{z}{\kappa^b_k[t]}\big) * f^e_k[t]\big(\frac{z}{\kappa^e_k[t]}\big)\Bigg), \end{aligned} \tag{21}$$

$$\begin{aligned} g^{\phi^V}_i[t](z) \triangleq{}& \gamma^u_i[t]\prod_{l\in\mathcal{N}}\Big(\gamma^b_{(l,i)}[t]\gamma^e_{(l,i)}[t]\Big) f^u[t]\big(\gamma^u_i[t]z\big) \\ &* \Bigg(\mathop{\circledast}_{l\in\mathcal{N}} f^b_k[t](\gamma^b_{(l,i)}[t]z) * f^e_k[t](\gamma^e_{(l,i)}[t]z)\Bigg). \end{aligned} \tag{22}$$

The proof of Theorem 1 and the definition of coefficients $\zeta^u_{(i,j)}$, $\gamma^b_{(l,i)}[t]$, $\gamma^e_{(l,i)}[t]$, and $\gamma^u_i[t]$ are given in Appendix I. Here, we do not make *any* assumption about the distribution of random parameters. Specifically, we do *not* assume any pre-determined PDF, such as Gaussian distribution. The discrete convolution in Theorem 1 can be calculated efficiency, e.g., using the methods in [39]. A brief discussion on the computational complexity of these convolution operations is given in the Section IV-D.

C. Design Implications

The results in Theorem 1 can be used to analytically, yet accurately, model the complex probability distributions of line power flows and voltage buses. An example is shown in Fig. 2. Here, we compare two methods. First, the proposed analytical method where we obtain the non-parametric distributions of operational parameters from the numerical convolution in Theorem 1. Second, the Monte-Carlo Simulation (MCS) method, where *extensive scenario generations* from the original random variables are applied to the power flow model in (1)-(3). We can see that the PDFs obtained from Theorem 1, achieve the same results as the MCS method. However, the computation complexity of our analytical method is much less than that of the MCS method, see Section IV-D.

III. Optimal Operation and Deployment of Energy Storage Units

The analytical approach in Section II can also be used to find the best charge and discharge schedules for the ESS in an optimization-based framework, as we will see in details next.

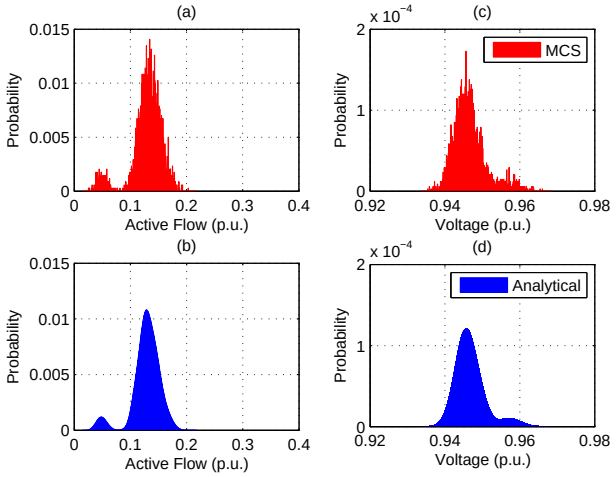

Fig. 2. Example non-Gaussian PDFs for the parameters of the network in Fig. 1: (a) and (b) power flow in line $(6, 10)$; (c) and (d) voltage at bus 10.

A. Bus Voltage Violation Chance Constraints

At each time slot, the probability of under- and over- voltage violations must be less than a certain threshold $\epsilon > 0$:

$$\begin{aligned} &\Pr\Big\{V_i[t] \le \underline{v}\Big\} < \epsilon \quad \Rightarrow \quad F^V_i[t](\underline{v}) < \epsilon, \\ &\Pr\Big\{V_i[t] \ge \overline{v}\Big\} < \epsilon \quad \Rightarrow \quad 1 - F^V_i[t](\overline{v}) < \epsilon. \end{aligned} \tag{23}$$

From (19), we can rewrite (23) as

$$\begin{aligned} &G^{\phi^V}_i[t]\Big(1 - \underline{v} - \psi^V_i[t]\Big) > 1 - \epsilon, \\ &G^{\phi^V}_i[t]\Big(1 - \overline{v} - \psi^V_i[t]\Big) < \epsilon. \end{aligned} \tag{24}$$

Since, by definition, $G^{\phi^V}_i[t]$ is a non-decreasing function, we have unique equivalents for (24) as follows [40]:

$$\begin{aligned} &1 - \underline{v} - \psi^V_i[t] > \sup\{\phi | G^{\phi^V}_i[t](\phi) \le 1 - \epsilon\}, \\ &1 - \overline{v} - \psi^V_i[t] < \inf\{\phi | G^{\phi^V}_i[t](\phi) \ge \epsilon\}. \end{aligned} \tag{25}$$

The right-hand sides in (25) are known, as long as $G^{\phi^V}_i[t]$ is known. Since $\psi^V_i[t]$ is a linear function of the ESS active and reactive power variables, the constraints in (25) are linear.

B. Line Active Power Flow Violation Chance Constraints

Next, we set the constraints to limit the probabilities of violating line thermal limits based on the line power flows:

$$\begin{aligned} &\Pr\Big\{P_{(i,j)}[t] \ge \overline{p}\Big\} < \epsilon \;\Rightarrow\; F^P_{(i,j)}[t](\overline{p}) > 1 - \epsilon, \\ &\Pr\Big\{P_{(i,j)}[t] \le \underline{p}\Big\} < \epsilon \;\Rightarrow\; F^P_{(i,j)}[t](\underline{p}) < \epsilon, \end{aligned} \tag{26}$$

and with the same analogy of Section III-A, we arrive at

$$\begin{aligned} &\overline{p} - \psi^P_{(i,j)}[t] > sup\{\phi | G^{\phi^P}_{(i,j)}[t](\phi) \le 1 - \epsilon\}, \\ &\underline{p} - \psi^P_{(i,j)}[t] < inf\{\phi | G^{\phi^P}_{(i,j)}[t](\phi) \ge \epsilon\}. \end{aligned} \tag{27}$$

C. Energy Storage System Operation Constraints

The operational constraints of the ESS can generally include many details, c.f. [41]. In this section, we discuss some of the basic, most dominant operational constraints of the ESS that are commonly adopted in the literature with respect

to tractable optimal operation. In particular, we address the constraints related to the ESS permissible energy and power charge/discharge constraints. The ESS power output limitations can be expressed as:

$$-I_i^s \leq P_i^s(t) \leq I_i^s, \tag{28}$$

where I_i^s denotes the power rating of the inverter.

Accurate energy reservoir constraints are also prominent in the ESS operation. Let $SoC_i[t]$ denote the energy that is available in the ESS at bus i during time slot t. The energy stored in the ESS should be maintained within the permitted upper and lower bounds; that is, we must have:

$$\begin{aligned} SoC_i[t] &\leq K_{cp}^{up} Ah_i \quad \forall i \in \mathcal{N}_S, \forall t \in \{1, \cdots, T\}, \\ SoC_i[t] &\geq K_{cp}^{dw} Ah_i \quad \forall i \in \mathcal{N}_S, \forall t \in \{1, \cdots, T\}. \end{aligned} \tag{29}$$

The energy that is stored (and available) in a battery at the end of time slot t, i.e. $SoC_i[t]$, is in fact a *non-linear, non-convex* function of the *vector* of all the power flows into and from the device since the beginning of operation until time slot t, i.e. $P_i^s[1], \cdots, P_i^s[t]$. Accordingly, given the available energy at the previous time slot, the state of charge at a time slot t, i.e. $SoC_i[t]$, can be stated as an iterative function of $SoC_i[t-1]$ and $P_i^s[t]$:

$$SoC_i[t] = SoC_i[t-1] + h(SoC_i[t-1], P_i^s[t]\Delta t). \tag{30}$$

The equality constraint in (30), however, includes a complex non-linear function of the battery's prior state of charge as well as the prior ESS charge/discharge rates. To handle this constraint in a *tractable* optimization, we *approximate* it as

$$SoC[t] = SoC[t-1] + h_{apx}(P_i^s[t]\Delta t). \tag{31}$$

Note that, $h_{apx}(\cdot)$ itself could still take a non-linear form in order to capture the impact of battery *efficiency* during each charge and discharge half-cycle. We use the model in [42]:

$$h_{apx}(P_i^s[t]\Delta t) = \begin{cases} 1/\eta_0 P_i^s[t]\Delta t & \text{if } \ P_i^s[t] \geq 0, \\ \eta_0 P_i^s[t]\Delta t & \text{if } \ P_i^s[t] < 0. \end{cases} \tag{32}$$

We can equivalently rewrite (32) as

$$h_{apx}(P_i^s[t]\Delta t) = \max\{\eta_0 P_i^s[t], 1/\eta_0 P_i^s[t]\}\Delta t. \tag{33}$$

More complex models, such as piece-wise linear approximations combined with binary variables can also be used to capture the dependency of $h_{apx}(P_i^s[t]\Delta t)$ to charge and discharge rates, e.g., see [43].

D. Energy Storage System Deployment Constraints

If we seek to select the best location(s) to install the storage unit(s), then we need to also define a variable $d_i \in \{0, 1\}$ which indicates whether or not an energy storage unit is installed at each bus i. Hence, the following constraints must hold:

$$Ah_i \leq d_i \cdot \overline{Ah}, \tag{34}$$

$$I_i^s \leq d_i \cdot \overline{I^s}, \tag{35}$$

$$\sum_{i \in \mathcal{N}} Ah_i \leq \overline{Ah}, \tag{36}$$

$$\sum_{i \in \mathcal{N}} I_i^s \leq \overline{I^s}, \tag{37}$$

$$\sum_{i \in \mathcal{N}} d_i = N_{ESS}. \tag{38}$$

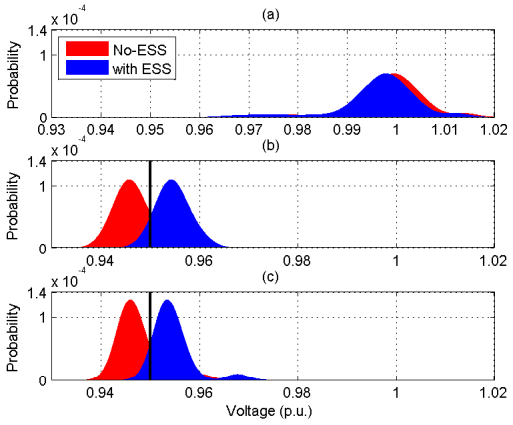

Fig. 3. The pdf of voltage at bus 10 with and without installed ESS: (a) The ESS is charged during time slot 8, which is an off-peak hour, and this has resulted in some tolerable drop in voltage; (b) The ESS is discharged during time slot 22, which is a peak hour, and this has resulted in some desirable increase in voltage; (c) The ESS is discharged also during time slot 24, which is another peak hour, and this has resulted in some desirable increase in voltage. The probability of violating the minimum threshold $\underline{v} = 0.95$ at hour 22 reduces from 0.7 to only 0.1 when the ESS is being used.

E. Energy Storage System Design Objective

Various design objectives can be considered when it comes to installing energy storage units on a distribution grid, e.g., see [19]. However, since the focus in this paper is on understanding the impact of using non-parametric stochastic optimization in energy storage planning, we account only for a typical design objective. Specifically, we seek to minimize

$$\sum_{i \in \mathcal{N}} \left(\sum_{t=1}^{T} \pi_{opr} \cdot |h_{apx}(P_i^s[t])| \right) + \pi_{cap} \cdot Ah_i + \pi_{inv} \cdot I_i^s. \tag{39}$$

The first term is related to the *operation* cost, i.e., the wear cost, which is proportional to the charge/discharge level at each time slot. The second and third terms are related to the *installation* cost, which are proportional to the size of the ESS.

F. Optimization Summary

In brief, the ESS optimization problem is formulated as

$$\begin{aligned} &\underset{P_i^s[t], E_i^s[t], Ah_i}{\textbf{Minimize}} \quad (39) \\ &\textbf{Subject to} \quad (25), (27), (28), (29), (31), (33) \\ &\qquad\qquad\ \ (34), (35), (36), (37). \end{aligned} \tag{40}$$

All the constraints in Sections III-A, III-B, and III-C are linear. The absolute-value function in the first term of the objective function in (39) can be replaced by linear constraints using auxiliary variables, c.f. [44]. Therefore, depending on whether the constraints in Sections III-D are taken into consideration, the formulated optimization problem is either a *linear program* or a *mixed-integer linear program.*

IV. Case Studies

Again, consider the distribution grid in Fig. 1. This grid represents the IEEE 13-bus distribution test feeder which is slightly modified. The feeder is assumed to be balanced. The additional parameters and data of this test network are given in [45]. The baseload is synthesized by aggregating the metered

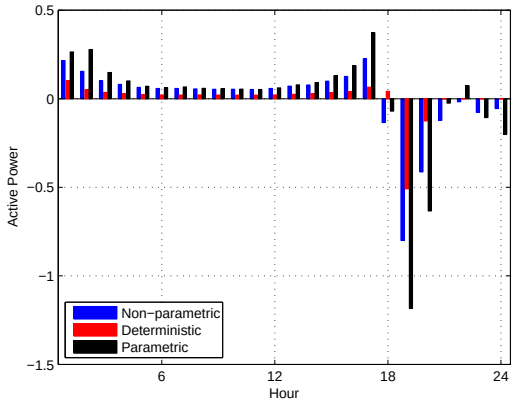

Fig. 4. The hourly ESS operation schedule based on three optimal designs.

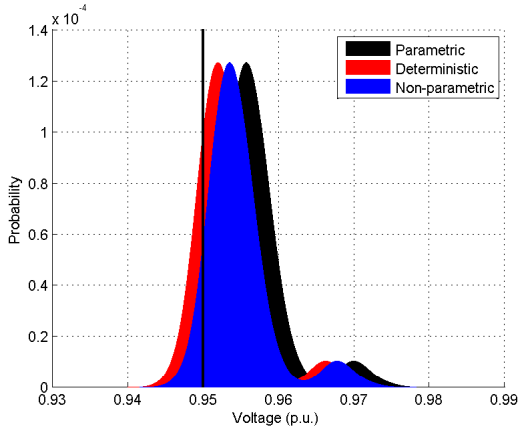

Fig. 5. The pdf of voltage in bus 10 at hour 24, under three different design approaches for the case study in Section IV.A.

hourly loads of 633 residential consumers in the PECON project [46], from January 2012 to August 2014. This is done such that the average combined load at each bus roughly matches its original feeder load in [47]. The generation output of a solar panel is synthesized by applying the metered pair of solar irradiation and temperature to a detailed dynamic model of a 1.2 MW solar panel in PSCAD [48]. The solar irradiation and temperature data was obtained from the LLNL database over six years form 2008 to 2013 for the months of May and June [49]. The hourly load of EV charging stations are from [6]. Given the focus of this paper, we take the PDFs of the random variables, e.g., solar generation, baseload, EV charging, etc. as given. These PDFs are obtained using the above historical hourly data.

The cost of battery is calculated for WB-LYP1000AHA lithium ion 1000 Ah battery modules with 3.2V discharge voltage [50]. The batteries operate between 20% to 80% of their nominal capacity. The rated lifetime of these batteries is 12,000 cycles and the current market price is $1,660 per module. Therefore, by dividing the module price by

$$2 \times Ah \times volts \times cap(\%) \times N_{cycle}, \tag{41}$$

we can estimate the battery wear cost as 36 $/MWh per cycle.

A. Parametric versus Non-Parametric Design

We compare our Non-Parametric Chance-Constrained (NPCC) approach with two other approaches in ESS planning: 1) Deterministic, where all random variables are represented by their mean values; 2) Parametric chance-constrained (PCC), where all random variables are represented by their Gaussian approximations, i.e., based on their mean and variance.

We start off our analysis based on a simplified problem set up, where the line power flow limits are not enforced, and only the bus voltage limits are considered. The minimum voltage threshold is assumed to be 0.95 per unit. The acceptable probability of violating the minimum voltage threshold is $\epsilon = 0.1$ or less. We consider the typical scenario where the battery system does not provide reactive power support. The location of the storage unit is assumed to be fixed at bus 7.

The probability mass functions of voltage at bus 10 are shown in Fig. 3, where there is severe voltage drop at peak hours prior to using ESS. The voltage distributions in one off-peak hour, hour 8, and two peak hours, hours 22 and 24 are shown prior and after ESS compensation. We can see that the use of ESS reduces the probability of violating the minimum threshold at peak hours. The probability of violating $\underline{v} = 0.95$ in bus 10 at hour 22 prior to ESS installation is 0.7. Such probability reduces to only 0.1 once the ESS is installed.

Next, we show the ESS operation schedules for various designs in Fig. 4. We can see that different designs lead to significantly different charge and discharge schedules. Accordingly, the obtained optimal size of the ESS is also different for each design. Based on the deterministic approach, it is presumed that the system constraints are met most of the time, thus *under-estimating* the potential for voltage violations. Accordingly, the size of the ESS unit is under-estimated and the allocated ESS unit is not used extensively. On the contrary, the PCC approach *over-estimates* the potentials for voltage violations. As a result, the ESS utilization based on PCC approach is higher than the NPCC approach in most peak hours. The required ESS capacity is also larger. Note that, the optimal ESS size based on the deterministic, PCC, and NPCC design approaches are 1.05, 3.57, and 2.69 MWh, respectively.

The voltage distributions for the deterministic, PCC, and NPCC designs are shown in Fig. 5. We can see that the deterministic approach compensates for the voltage less than the NPCC approach, whereas the PCC approach compensates more than the NPCC approach at this hour. The probability that the voltage distribution falls below $\underline{v} = 0.95$ is 0.21, 0.093, and 0.018 for the deterministic approach, the NPCC approach, and the PCC approach, respectively.

Additional details about the ESS operation during time slots 22 and 24 based on the PCC approach are given in Fig. 6. Here, the Gaussian approximations of the voltage probability functions with and without ESS unit are compared with the empirical pdf curves. The approximated probability of voltage violation, i.e., the black shaded area in Fig. 6(a), is 0.07. However, the empirical probability of voltage violation is only 0.02 in Fig. 6(b). This confirms our previous observation that a PCC approach often over estimates the probability of voltage violation; thus, requiring a ESS size larger than what is actually needed. The inaccurate estimation of the probability of violating the voltage constraints is the main reason for the difference between the PCC approach and the NPCC approach.

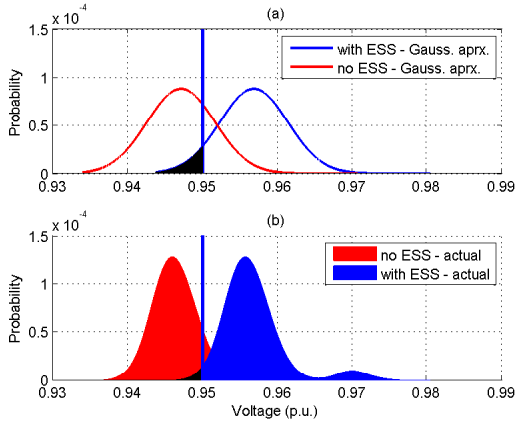

Fig. 6. Voltage compensation at hour 24 based on the PCC approach: (a) the Gaussian approximation of the voltage pdfs; (b) the true voltage pdfs.

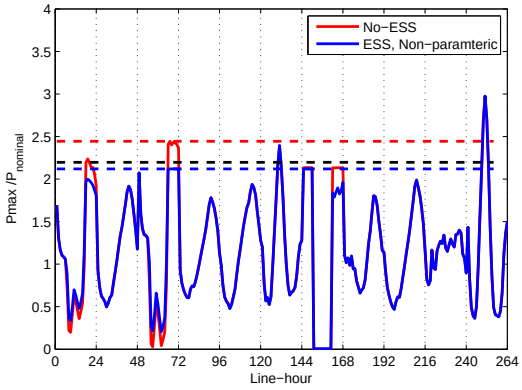

Fig. 8. The best maximum active power flow bounds achieved during $11 \times 24 = 264$ line-hour instances under NPCC approach.

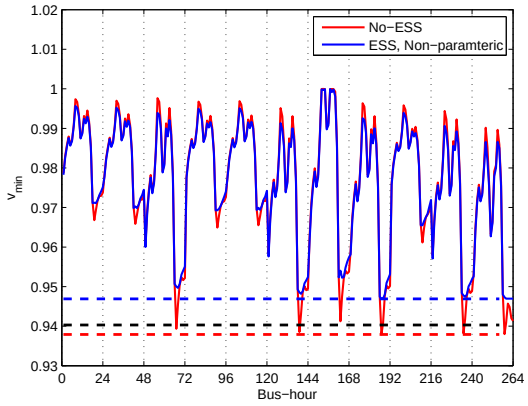

Fig. 7. The best minimum voltage bounds achieved during $11 \times 24 = 264$ bus-hour instances under NPCC approach.

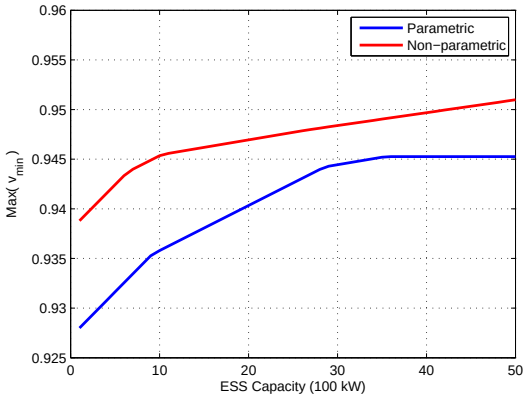

Fig. 9. The maximum $\underline{v}$ bounds achieved in all buses for different ESS capacities under NPCC and PCC design approaches.

B. Compensation on System Operational Limits

In this section, we discuss another factor that further shows the advantages of NPCC over PCC. First, we note the fact that an ESS cannot increase the voltage or decrease the power flow at a certain hour, *unless it decreases the voltage and increases the power flow at another hour*. Therefore, the distribution network must originally be capable of tolerating bus voltage decreases or line power flow increases during certain hours; otherwise the ESS is *not* the solution for alleviating the system undesirable states. Therefore, next, we examine the system operational bounds under different ESS design approaches.

Unlike in Section IV-A, where the minimum threshold for voltages was pre-set to $\underline{v} = 0.95$, and the required ESS capacity was obtained using different approaches, in this section, we instead assume that the ESS storage capacity is fixed to $2MWh$ and we rather obtain the best voltage operation thresholds using non-parametric and parametric approaches. Same as in Section IV-A, we assume that $\epsilon = 0.1$.

To examine the system operational bounds, we introduce some slack variables to all chance constraints. That is, we treat the acceptable system state bounds in Sections III-A and III-B to be decision variables. Instead, we set the ESS capacity to be fixed. We also introduce a new *regulatory* term $K_{reg} \max_{i,t}\{\underline{v}_i[t]\}$ into the objective function in (39), where K_{reg} is a large weight factor. The purpose of adding this regulatory term is to make all chance constraints binding so that we can obtain the best bounds achievable for each state.

Fig. 7 shows the tolerable bounds for the case of bus voltage compensation when the proposed NPCC approach is used. The blue dashed line shows the minimum of such bounds across all locations and all time slots. Here, we also show the similar minimum bounds for the PCC and the No-ESS case. In this figure, if the minimum bound is 0.94 p.u. with at least 90% probability at all times, then the PCC approach gives an *infeasible solution* with 2 MWh of ESS at bus 8.

A similar analysis can be done to assess the tolerable bounds for line power flow compensation. Here, we must minimize the power flow on the most congested line. To do so, we shall minimize the maximum of $\overline{p}/p_{nominal}$ for each line. The results are shown in Fig. 8. We can see that the ESS compensation brings down the highest power flow limit. However, the ESS may affect only the lines that lie on the path from the ESS to the substation bus. Therefore, the ESS location is of importance if we intend to lower the power flow on a particular line. For each ESS capacity, this figure also shows how much the maximum power flow can be reduced by the ESS among the lines that *have the possibility of improvement based on the ESS location.*

The best minimum voltage bounds achieved in 24 hours at

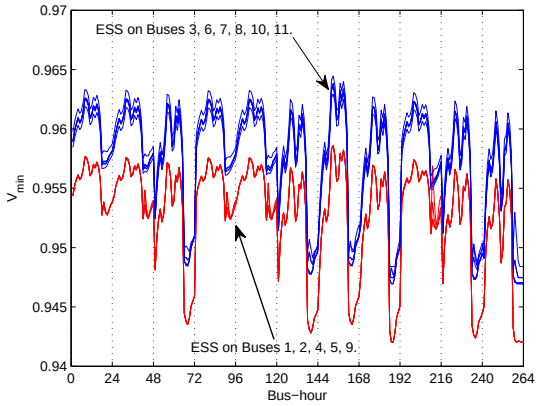

Fig. 10. The Impact of ESS location on voltage improvement at each bus.

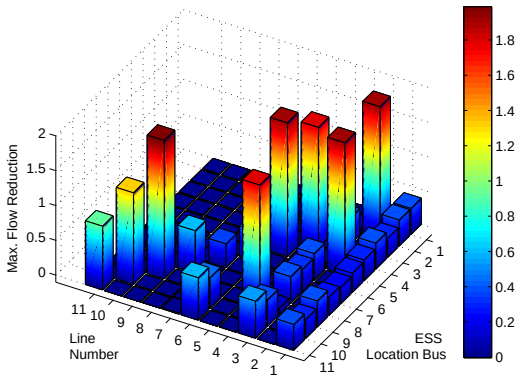

Fig. 11. The impact of ESS location on active flow improvement at each line.

all buses as a function of ESS capacity under NPCC and PCC stochastic design approaches are shown in Fig. 9. First, we note that both curves are continuous, piecewise linear, concave, and monotonic increasing, c.f. [51, Lemma 2]. Second, we can see that the NPCC approach can always enforce higher minimum voltage, regardless of the capacity of the ESS.

C. Impact of Location

Next, we take a closer look at the impact of the ESS location on improving the system tolerable bounds that we introduced in Section IV-B. This also brings up the question on optimizing the location, when there are multiple ESS units.

We observe in Fig. 10 that installing an ESS at either of buses 1, 2, 4, 5, and 9 does not significantly improve the minimum voltage bounds. Therefore, at least for the purpose of voltage improvement, these buses are *not* suitable locations for ESS installation. Note that, we do not suffer from over-voltage issue of PV injections at end buses since the grid is heavy-loaded.

Based upon a similar analysis as in Section IV.B, Fig. 11 shows the normalized maximum active power flow bound reduction in each line, i.e. $\Delta\overline{p}$ for the cases of *with* and *without* ESS installation. We can see that installing the ESS at each bus improves the active power flow only on certain lines in the path between the ESS bus and the reference bus. Since the back current issue is not considered, installing an ESS is always preferred in the end buses of a heavy-loaded line.

D. Optimal Locations and Sizes of Multiple ESS Units

Recall that in sections IV-A to IV-C, only a single ESS unit was deployed and the optimization did not involve choosing the location of the ESS. As we illustrated in Section IV-C, however, the location of the ESS unit can have a significant impact on its ability to improve the system operational parameters. Additionally, the *locations of uncertain resources* in the distribution system can also have impact on the ESS requirements for the system. Therefore, we obtained the optimal ESS locations and sizes for the base-case as well as for several additional test cases, where the location of some random resources are changed in the test distribution system of Fig. 1. The results of the optimal deployment solutions for the NPCC and PCC approaches are given in Table I for two ESS units (i.e. $N_{ess} = 2$). Note that, the ESS units are deployed in order to maintain the voltage violation probabilities within 10% of the thresholds as in Section IV-A.

TABLE I
OPTIMAL LOCATIONS AND SIZES FOR TWO ESS UNITS

Case Number	PV Bus	EV Chargers Buses	Optimal ESS Plan			
			Capacity (MWh)		Bus Location	
			NPCC	PCC	NPCC	PCC
1	7	7,8,9	1.6,0.33	0.12, 3.2	8, 11	8,10
2	3	2,4,11	0.29, 0.03	0.31,0.02	8,10	8,10
3	4	2,3,6	0.38, 0.08	0.5,0.3	8,10	10,11
4	1	4,5,7	0.32, 0.01	0.13,0.21	8,10	7, 8

From the results in Table I, we can make several observations. First, the NPCC method achieves a better solution in terms of a lower deployed ESS capacity to maintain the same voltage thresholds. The overall ESS capacity deployed by NPCC is 1.93 MWh, whereas PCC requires the deployment of 3.32 MWh ESS capacity. Second, the deployed capacity with multiple ESS units and in the optimal locations is smaller both in NPCC and PCC approaches compared to Section IV-A, where the location of the single ESS was arbitrarily selected. Third, the choice of the design method, i.e., NPCC or PCC, in representing the random variables can have an impact on the optimal locations of ESS unit as well. Specifically, from case numbers 2-4 in Table I, it is also observed that the required ESS capacity as well as the optimal ESS locations are greatly affected by the locations of the random resources on the distribution system. In Case 1, the placement of those resources at the end buses has led to more voltage drops and hence more ESS capacity requirements. In contrast, in Cases 2 to 4, we have less ESS requirements, because several random resources are placed in up-stream buses of the distribution grid. Finally, the design objective towards which the ESS deployment is optimized, e.g. better voltage compensation, lower line power flow reduction, and/or reverse flow prevention, has great impact on the choices of the ESS capacity and locations.

E. Comparison with Scenario-Based Stochastic Optimization

In this section, we compare the performance of our proposed NPCC approach with that of the methods that rely on sampling

of input random variables. To this aim, we approximate the chance constraints in (25) and (27) with some convex bounds in the form of their expected values, specifically by using the Markov Bounds [52]. We then compare the two approaches for the same set-up and objectives of Section IV-A.

TABLE II
OPTIMAL LOCATIONS AND SIZES FOR TWO ESS UNITS TO MITIGATE THE VOLTAGE VIOLATION.

Method	Decision Vars. Num.	ESS Cap. (MWh)	Voltage Violation Worst Probability
NPCC	97	2.69	0.105
SBO(50)	55800	6.25	0.112
SBO(100)	217800	5.5	0.086
SBO(500)	1M+	4.1	0.073

The optimal ESS capacity deployed by each approach to maintain the system voltage within the 90% tolerable range is compared for each approach, and the results are shown in Table II. Here, the scenario-based optimization (SBO), solved with 50 scenarios, converges roughly within the same time that our proposed approach converges, including its distribution processing time. However, the deployed ESS capacity to maintain the voltage violations within the probability threshold, is much higher for SBO than the NPCC approach, which means a *better resource management* for our proposed NPCC approach.

We also compared the actual numerically-obtained probability of voltage violation for each method using Monte-Carlo simulation with 10,000 random scenarios. The worst probability of voltage violation across the system buses and at different hours is shown in Table. II. We observe that SBO with 50 scenarios leads to even a higher probability of violation, even with a larger ESS capacity deployed. We also see in Table II that the performance of SBO indeed improves with a larger number of scenarios. However, such improvement is obviously at the expense of higher computational complexity. Another observation was that increasing the number of scenarios is not *easy*, because as we increase the number of scenarios, the performance of the scenarios-based optimization approach either becomes dependent to the choice of solver software or all solvers face *numerical issues* to reach a solution.

We note that, there exist techniques, e.g those in [53]–[55], to decompose and / or improve the computation efficiency of scenario-based optimization approaches. They often are applicable to a wide range of optimization problems, including our intended problems, and are independent of the inherent computation burden of solving the optimization problem under many instances of the random variables. However, those techniques are *not* always guaranteed to convergence.

F. Computational Complexity and Accuracy

In this section, we assess the impact of the common DistFlow model linearization on the result accuracy. Fig. 12 compares the empirical voltage PDFs obtained from Theorem 1 and that of a Monte-Carlo Simulation that is based on *non-linear power flow equations*. We can see that due to ignoring the line losses, the analytical voltage PDFs are slightly different from the empirical PDFs. Thus, there is a small over estimation in the voltage PDFs when the linear flow

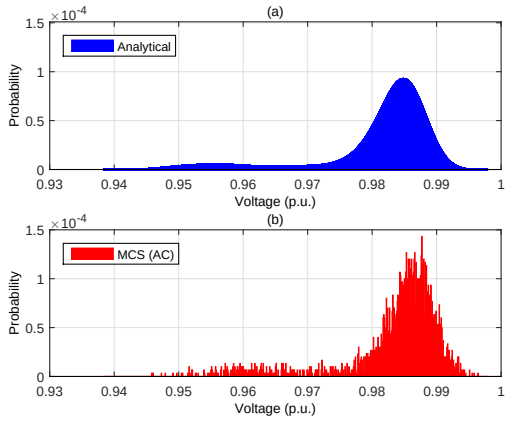

Fig. 12. Power flow linearization impact on a voltage distribution at hour 17.

model is used. However, the significantly lower computation complexity of our analytical method compensates its slight inaccuracy. For example, in Fig. 12, we perform only 12 convolution operations to obtain the voltage PDF in each bus, whereas more than $60,000$ scenarios are generated to construct the empirical PDF.

We also compared the computation efficiency of our proposed approach with those of the two existing approaches. The results are shown in Table III. Note that, our proposed approach consists of two parts: first, an analytical stochastic representation of the operational parameters, i.e. bus voltages and line active and reactive flows; and second, a chance-constrained optimization approach based on the results in the first part. The computation time required for the first part is compared to that of the Monte-Carlo simulation method discussed in section II-C with 60,000 scenarios to produce comparable resolution of operational parameters probability density functions. The amount of computation time required for MCS is more than 500 times that of our proposed analytical approach. The overall runtime of our proposed approach, i.e. for the first as well as the second part mentioned earlier, is also compared with that of scenario-based stochastic optimization (SBO), discussed in section IV-E, with a mere 100 scenarios. Clearly, in order to increase the accuracy of the scenario-based optimization approach, the required computation time increases significantly. The runtime obtained for all the methods above is based on a single 2.67 GHz processor.

TABLE III
THE COMPUTATION TIME REQUIRED FORM DIFFERENT METHODS.

Method	Analytical	Monte-Carlo	NPCC	SBO
Runtime (min.)	37	20000	90	225

The convolution operations required to obtain *each* operational parameter is at most equal to the number of independent random variables. It does *not* depend on network size. Also, for a practical system, we may not need the PDFs of all operational parameters, but just for a few important ones. To assess the computation efficiency, in the data preparation process, the hourly PDFs of more than 500 individual residential users with length of 60 for each vector, i.e., 12,000 operations in total, was convolved in only few minutes using a single processor.

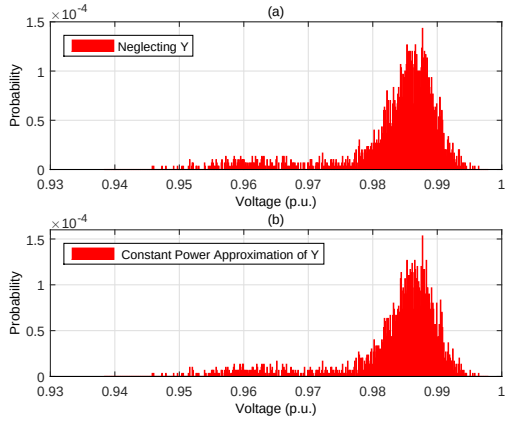

Fig. 13. The voltage distribution at bus 11 and hour=17, which are obtained using MCS with 60,000 scenarios and AC power flow model: (a) the line transverse parameters (Y) are neglected; (b) Those parameters are modelled as constant power shunt elements.

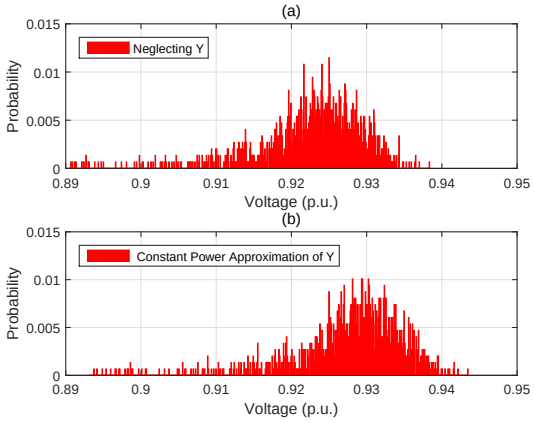

Fig. 14. The voltage distribution at bus 11 of IEEE 34-bus test feeder (weak grid) and hour=17, which are obtained using MCS with 30,000 scenarios and AC power flow model: (a) the line transverse parameters (Y) are neglected; (b) Those parameters are modelled as constant power shunt elements.

G. Impact of Line Traverse Parameters

Next, we examine the impact of considering the distribution line transverse parameters, such as the capacitances of coaxial cables, on the probability distributions of the operational parameters, e.g. bus voltages. Based on the presented formulation in section II-B, the impact of transverse line parameters may not be modeled thoroughly due to the limitations of the DistFlow model. There are often two approaches to take with respect to this issue. First, in many studies, the impact of transverse line parameters are simply *neglected*, such as in [33], [56]. Note that, the results in Sections IV-A to IV-F are similarly obtained by neglecting the impact of transverse line parameters. Second, there are studies that try to *approximate* the impact of transverse line parameters, by modeling them as constant power shunt elements connected to the terminal buses of each line. This second approach is tried in Fig. 13, where we compare the results of bus voltage distribution at bus 11 and hour 17, for two cases. The first case is where the impact of transverse line parameters are neglected. The second case is where such parameters are approximated as constant power elements. The results are obtained from MCS with 60,000 scenarios. The AC power flow equations are solved by applying second-order cone programming, c.f. [36].

We see in Fig. 13 that the voltage distribution inaccuracy due to neglecting the line suscpetance is *not* significant. The reactive power injections from the lines shunt capacitors are well below $8{\times}10^{-4}$ p.u. in all buses. It is presumed the results inaccuracy due to *inability* of Distflow model in representing lines constant impedance capacitance, instead of constant power, is even *less* significant.

However, the results in Fig. 13 for the distribution grid of Fig. 1, may not be generalized to *all* distribution grids. In particular, in case of *weak* distribution systems with long feeders, the impact of transverse line parameters could in fact be noteworthy and have impact on calculating the bus voltage and line flow violation flow constraints. For instance, in Fig. 14, we evaluated the impact of neglecting the line transverse parameters for a weaker network, i.e., a modified IEEE 34 bus distribution grid. Again, the distributions of a single bus voltage at a given hour were compared in two cases where transverse line parameters are neglected or alternatively modeled as constant power elements. The additional parameters of this test network are given in [45]. Note that the same MCS method of Fig. 13 is applied here on the 34 bus grid. We can see in Fig. 14, that if the impact of the transverse line parameters are neglected, then the calculated voltage of the selected bus is lower than the actual voltage values. Therefore, for a week network such as the one in Fig. 14, it is advised to consider the impact of such parameters. We emphasize that, the probability distribution depicted in Fig. 14 is still not an entirely accurate representation of the true bus voltage values where transverse line parameters are accurately modeled. Even though, with *approximating* the transverse line parameters as constant power components, the inaccuracy of the *DistFlow model* is significantly mitigated, such model is still unable to account for the quadratic voltage-dependency of reactive power injections of line shunt capacitances. Thus, such inaccuracy needs to be accounted for in the final design.

H. Multiple-year Chance-constrained Design

Finally, in this section, we utilize our proposed non-parametric probabilistic approach in conducting a multiple-year time horizon planning based on operational chance-constraints. Note that, the objective function that we introduced in (39), and applied so far for the results discussed in sections IV-A to IV-G, is covering the typical, most essential cost model in ESS operation problem. However, in a detailed ESS planning problem, it is suitable to also consider a multiple-year time horizon design which accounts for future grid conditions. Such design would have to incorporate large time series of stochastic variables. It will also involve the forecast of the grid stochastic load and generation growth. Therefore, here we present an analysis of ESS planing with considering multi-year time horizon planning performed via parametric and non-parametric chance-constrained optimization. We shall emphasize, however, that a comprehensive ESS planning design would involve many details, which are not within the scope of this paper.

To form a new objective function for the purpose of a multi-year planning design, we first represent the ESS installed

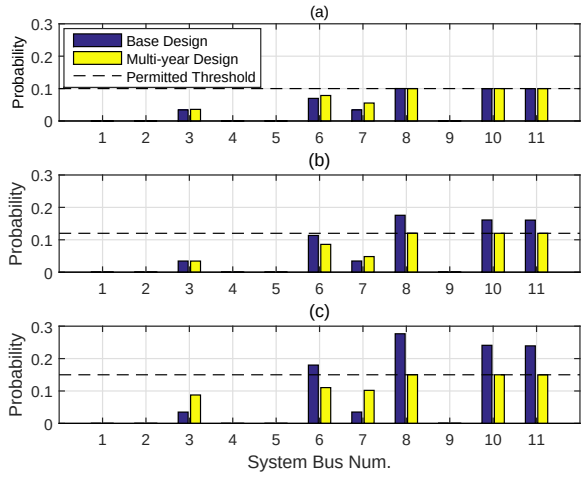

Fig. 15. The probabilities of bus voltage violations under single-year and multi-year ESS planning; the daily largest values at (a) year one, (b) year two, and (c) year three.

capacity, i.e. I_i^s, and Ah_i^s, based on the operation schedules obtained for multiple years. The operating schedules are obtained to maintain system operational constraints in the successive years of the design horizon. Therefore, we form the multi-year design objective as

$$\sum_{i\in\mathcal{N}}\Bigg(\pi_{cap}\cdot Ah_i+\pi_{inv}\cdot I_i^s+ \sum_{yr=1}^{N_{year}}\sum_{t=1}^{T}\pi_{opr}^{yr}\cdot|h_{apx}(P_i^s[t,yr])|\Bigg), \tag{42}$$

where π_{opr}^{yr} denotes the operational cost coefficient for each year within the design horizon. Here, we assume that the design horizon is three years. More details regarding the ESS installation and operation costs can be found at studies such as [57], [58]. Note that, we have also some additional *system constraints* in order to maintain the acceptable operation conditions in each year of the design horizon. Accordingly, functions $\psi_i^V[t]$, $\psi_{i,j}^P[t]$, $G_i^{\phi^V}[t]$, and $G_i^{\phi^P}[t]$ in (25) and (27) are extended to $\psi_i^V[t,yr]$, $\psi_{i,j}^P[t,yr]$, $G_i^{\phi^V}[t,yr]$, and $G_i^{\phi^P}[t,yr]$, respectively. Additionally, since the uncertainty in grid random power injections increase as we move forward in time, it is reasonable to apply different violation probabilities for each year. Here, we assume that the allowed violation probability is 0.1, 0.15, and 0.2 for the first, second, and third years of the design horizon. We also assume that the random loads and random generations have a constant growth rate of α each year. Accordingly, in our model, the probability distributions of the input random variables representing power injections of the loads/generators are multiplied by a factor of $1+\alpha$ each year. Here, without loss of generality, we assumed the growth factors of 1 %, 2 %, and 5% for the EV chargers, residential baseload, and PV generation, respectively.

Te performance of ESS planing based on the aforementioned multi-year design is compared with that of the base-design, i.e. based on the objective in (39). In both cases, the ESS is installed at bus 7 of the distribution grid in Fig. 1. The ESS capacity and the yearly operation schedules are obtained based on each design. Fig. 15 shows the results. In this figure, the maximum probability of voltage violation in each bus is shown for the first, second and third years of the design horizon. We can see in Fig. 15 that the voltage violation probabilities are beyond the allowed values in the base design, where the impact of stochastic load growth is ignored. In the multi-year design, however, the stochastic load growth is considered; thus the capacity and the different operation schedules are calculated based on the multi-year design. The required ESS capacity is 3.56 MWh based on multi-year design. Accordingly, the voltage violations are kept within the permitted probabilities, in all three years of the design horizon. We can conclude that , our proposed non-parametric approach can readily be used in a multi-year planning framework.

V. Additional Remarks and Extensions

A. Modeling Chance-Constraints Based on Line Currents

In section III-B, the chance-constraints related to line flows were expressed in terms of power. However, in practice, for lines below 36 kV, this value is often expressed in terms of current. If one chooses to use a current-based model, he/she needs to transform our power-limit constraints to current-limit constraints, e.g., in form of $I^2 < I_{max}^2$. Since $I^2 = S^2/V$, such constraint can then be transformed into $S^2 \leq I_{max}^2 V$. If we neglect the changes in voltage, then after replacing S^2 with its active and reactive power terms, we have:

$$\Big\{P_{i,j}^2+Q_{i,j}^2<S_{max}^2.\Big\}>1-\epsilon. \tag{43}$$

If the ESS power injection is given, then we can obtain the distributions of $P_{i,j}$, $Q_{i,j}$, and $S_{i,j}$ in terms of ESS injections. But even in that case, the above family of constraints will not be convex. Note that, since $P_{i,j}=\psi_{i,j}^P+\phi_{i,j}^P$, for the square variable, we will have multiplication of random variables and decision variables, which renders the optimization non-convex when we use non-parametric distributions. Of course, a tractable chance-constraint on the current of the transmission line can still be *approximated*, possibly by using several independent linear constraints on active and reactive power flow of the line. Even by doing so, the dependency of the original chance constraints on the bus voltages are neglected. Based on the rated voltage of the distribution grid, and depending on how weak the gird is, parameter S_{max} in (43) could actually be lower than what is assumed. This approximation could potentially lead to some inaccuracies in the results obtained based on the current chance constraints. Therefore, the generalization of the proposed approach for the current chance-constraints may require further investigation. However, addressing this issue is beyond the scope of this paper. It could be a pointer for a future work.

B. Impact of Slack-Bus Voltage Variations

In order to study the stochastic representation of the model in Section II, we assumed that the voltage on the slack bus is fixed. However, in practice, this value might fluctuate as a function of the state of the upstream grid. The impact of slack

bus voltage fluctuations may as well be treated as a stochastic random variable, independent of the nodal power injections. By considering the slack bus voltage as a random variable with probability density function of f^{V_0}, we can write (9) as

$$F_i^V[t](v) \triangleq 1 - \Pr\Big\{\tilde{\phi}_i^V[t] - \tilde{V}_0 \leq -v - \psi_i^V[t]\Big\}, \quad (44)$$

which will result in the following CDF of voltage distributions:

$$F_i^V[t](v) = 1 - G_i^{\phi'^V}(-v - \psi_i^V). \quad (45)$$

Here $G_i^{\phi'^V}$ is the CDF corresponding to density function

$$g_i^{\phi'^V}(z) = -g_i^{\phi^V}(z) * f^{V_0}(-z). \quad (46)$$

VI. Conclusions

A non-parametric chance-constrained optimization approach was proposed for energy storage operation and planning in power distribution networks. The analysis was done by introducing new closed-form stochastic models for various key operational parameters, with no restricting assumption on the probably distribution of random parameters. Uncertainties from different sources of different nature, such as DGs and EVs, were considered. Several case studies confirmed the advantages of the proposed design method compared to the conventional deterministic and parametric (based on Gaussian approximation) chance-constrained optimization frameworks. In future, the developed closed-form stochastic models can be used in other non-ESS distribution-level planning problems. Some limitations of the proposed approach such as inaccuracy of the approximations in the chance constraints on line currents, and inaccuracy of the constraints on ESS energy reservoirs can as well be addressed in follow-up studies.

Appendix: Proof of Theorem 1

From the properties of linear transformations on density functions, c.f. [59], if $Y = a_1X_1 + \cdots + a_NX_N$, then

$$\begin{aligned} f_Y(y) &= f_{a_1X_1}(y) * \cdots * f_{a_NX_N}(y) \\ &= \left(\frac{1}{a_1} \cdots \frac{1}{a_N}\right) \cdot f_{X_1}(y/a_1) * \cdots * f_{X_N}(y/a_N). \end{aligned} \quad (47)$$

Therefore, the expression in (20) results directly from (11) and (16), where the coefficient $\zeta_{i,j}^u$ is defined by tracking all the DGs that are on descendants of the intended node:

$$\zeta_{(i,j)}^u \triangleq 1/\left(\sum_{k\in\mathcal{N}_j} \lambda_k^u\right). \quad (48)$$

We can show (21) similarly. Note that, since $\tilde{Q}_k^b = \kappa_k^b \tilde{P}_k^b$ and $\tilde{Q}_k^e = \kappa_k^e \tilde{P}_k^b$, we have

$$\begin{aligned} f_k^{Q^b}(z) &= (1/\kappa_k^b) f_k^b(z/\kappa_k^b), \\ f_k^{Q^e}(z) &= (1/\kappa_k^e) f_k^e(z/\kappa_k^e). \end{aligned} \quad (49)$$

Therefore, from (12), (16) , and (47), we can obtain (21).

To derive (22), we note that the distributions $\phi_{k,j}^P$ across $(k,j) \in \mathcal{L}_{i,0}$ are not independent. The distributions of $\phi_{k,j}^Q$ across $(k,j) \in \mathcal{L}_{i,0}$ are not independent either. Thus, we can rewrite (13) in terms of the original independent random variables f_k^b, f_k^e, and f^u. Specifically, from (11)-(13), we have:

$$\gamma_{(l,i)}^b[t] \triangleq 1\Big/\left(\sum_{(j,k)\in\mathcal{L}_{i,0}\cap\mathcal{L}_{l,0}} 2(R_{(j,k)} + X_{(j,k)})\kappa_l^b[t]\right), \quad (50)$$

$$\gamma_{(l,i)}^e[t] \triangleq 1\Big/\left(\sum_{(j,k)\in\mathcal{L}_{i,0}\cap\mathcal{L}_{l,0}} 2(R_{(j,k)} + X_{(j,k)})\kappa_l^e[t]\right). \quad (51)$$

For renewable DGs, since they are all assumed to depend on the similar solar irradiance, we combine the coefficients of all the DG's that share a path with the intended node:

$$\gamma_i^u[t] \triangleq 1\Big/\left(\sum_{l\in\mathcal{N}^s}\sum_{(j,k)\in\mathcal{L}_{i,0}\cap\mathcal{L}_{l,0}} \lambda_l^u\big(2(R_{(j,k)}+X_{(j,k)})\kappa_l^u[t]\big)\right) \quad (52)$$

References

[1] A. Nourai, "Installation of the first distributed energy storage system (DESS) at american electric power (AEP)," Sandia Report SAND2007-3580, Tech. Rep., June 2007.

[2] S. Shao, F. Jahanbakhsh, J. Aguero, and L. Xu, "Integration of PEVs and PV-DG in power distribution systems using distributed energy storage - dynamic analyses," in *Proc. of IEEE PES Innovative Smart Grid Technologies conference*, Washington, DC, Feb. 2013.

[3] a. T. R. F. Pieltain, R. Cossent, C. Domingo, and P. FriÌąas, "Assessment of the impact of plug-in electric vehicles on distribution networks," *IEEE Trans. on Power Systems*, vol. 26, no. 1, pp. 206–213, Feb 2011.

[4] D. Bienstock, M. Chertkov, and S. Harnett, "Chance-constrained optimal power flow: risk-aware network control under uncertainty," *SIAM Review*, vol. 56, no. 3, pp. 461–495, 2014.

[5] L. Bechini, G. Ducco, M. Donatelli, and A. Stein, "Modelling, interpolation and stochastic simulation in space and time of global solar radiation," *Agriculture, Ecosystems and Environment*, vol. 81, no. 1, pp. 29 – 42, 2000.

[6] H. Akhavan-Hejazi, H. Mohsenian-Rad, and A. Nejat, "Developing a test data set for electric vehicle applications in smart grid research," in *Proc. of IEEE VTC*, Vancouver, BC, Sept. 2014.

[7] S. Shenoy, D. Gorinevsky, and S. Boyd, "Non-parametric regression modeling for stochastic optimization of power grid load forecast," in *Proc. of IEEE American Control Conference*, Chicago, IL, July 2015.

[8] S. Shenoy and D. Gorinevsky, "Stochastic optimization of power market forecast using non-parametric regression models," in *Proc. of IEEE PES General Meeting Conference*, Denver, CO, July 2015.

[9] J. Dias and C. Borges, "A non parametric stochastic model for river inflows based on kernel density estimation," in *Proc. of Probabilistic Methods Applied to Power Systems Conference*, Durham, NC, July 2014.

[10] F. Chacra, P. Bastard, G. Fleury, and R. Clavreul, "Impact of energy storage costs on economical performance in a distribution substation," *IEEE Trans. on Power Systems*, vol. 20, no. 2, pp. 684–691, May 2005.

[11] G. Martin, "Optimal implementation of energy storage systems in power distribution networks," Master's thesis, University of Minnesota, Digital Conservancy, http://purl.umn.edu/132215, June 2012.

[12] G. Celli, S. Mocci, F. Pilo, and M. Loddo, "Optimal integration of energy storage in distribution networks," in *Proc. of IEEE Conference PowerTech*, Bucharest, Romania, June 2009.

[13] C. Thrampoulidis, S. Bose, and B. Hassibi, "Optimal placement of distributed energy storage in power networks," *arXiv:1303.5805*, 2013.

[14] S. Lin, M. Han, R. Fan, and X. Hu, "Configuration of energy storage system for distribution network with high penetration of PV," in *Proc. of IET on Renewable Power Generation*, Edinburgh, UK, 2011.

[15] A. Sjodin, D. Gayme, and U. Topcu, "Risk-mitigated optimal power flow for wind powered grids," in *Proc. of IEEE ACC*, Montreal, QC, June 2012.

[16] X. Xi, R. Sioshansi, and V. Marano, "A stochastic dynamic programming model for co-optimization of distributed energy storage," *Energy Systems*, vol. 5, no. 3, pp. 475–505, Sept. 2014.

[17] M. Ding and X. Wu, "Three-phase probabilistic power flow in distribution system with grid-connected photovoltaic systems," in *Proc. of IEEE APPEEC*, Shanghai, China, Mar. 2012.

[18] S. Al-Kaabi, H. Zeineldin, and V. Khadkikar, "Planning active distribution networks considering multi-DG configurations," *IEEE Trans. on Power Systems*, vol. 29, no. 2, pp. 785–793, Sept. 2014.

[19] M. Nick, R. Cherkaoui, and M. Paolone, "Optimal allocation of dispersed energy storage systems in active distribution networks for energy balance and grid support," *IEEE Trans. on Power Systems*, vol. 29, no. 5, pp. 2300–2310, Feb. 2014.

[20] S. Huang, J. Xiao, a. G. R. J. Pekny, and A. Liu, "Quantifying system-level benefits from distributed solar and energy storage," *Journal of Energy Engineering*, vol. 138, no. 2, pp. 33–42, June 2011.

[21] C. Abbey and G. Joos, "A stochastic optimization approach to rating of energy storage systems in wind-diesel isolated grids," *IEEE Trans. on Power Systems*, vol. 24, no. 1, pp. 418–426, Dec. 2009.

[22] M. Fan, V. Vittal, G. T. Heydt, and R. Ayyanar, "Probabilistic power flow analysis with generation dispatch including photovoltaic resources," *IEEE Trans. on Power Systems*, vol. 28, no. 2, pp. 1797–1805, 2013.

[23] N. Yang and F. Wen, "A chance constrained programming approach to transmission system expansion planning," *Electric Power Systems Research*, vol. 75, no. 2âĂŞ3, pp. 171 – 177, Aug. 2005.

[24] A. Geletu, M. Kloppel, H. Zhang, and P. Li, "Advances and applications of chance-constrained approaches to systems optimisation under uncertainty," *Journal of Systems Science*, vol. 44, 2013.

[25] M. Kloppel, A. Gabash, A. Geletu, and P. Lii, "Chance constrained optimal power flow with non-gaussian distributed uncertain wind power generation," in *Proc. of IEEE International Conference on Environment and Electrical Engineering*, Wroclaw,Poland, May 2013.

[26] A. Schellenberg, W. Rosehart, and J. Aguado, "Cumulant-based probabilistic optimal power flow with gaussian and gamma distributions," *IEEE Trans. on Power Systems*, vol. 20, no. 2, pp. 773–781, May 2005.

[27] A. Tamtum, A. Schellenberg, and W. Rosehart, "Enhancements to the cumulant method for probabilistic optimal power flow studies," *IEEE Trans. on Power Systems,*, vol. 24, no. 4, pp. 1739–1746, Nov 2009.

[28] B. Zeng, J. Zhang, X. Yang, J. Wang, J. Dong, and Y. Zhang, "Integrated planning for transition to low-carbon distribution system with renewable energy generation and demand response," *IEEE Trans. on Power Systems*, vol. 29, no. 3, pp. 1153–1165, May 2014.

[29] Z. Liu, F. Wen, and G. Ledwich, "Optimal siting and sizing of distributed generators in distribution systems considering uncertainties," *IEEE Trans. on Power Delivery*, vol. 26, no. 4, pp. 2541–2551, 2011.

[30] A. Darvishi, A. Alimardani, and B. Abdi, "Optimized fuzzy control algorithm in integration of energy storage in distribution grids," *Energy Procedia*, vol. 12, pp. 951 – 957, 2011.

[31] V. Evangelopoulos and P. Georgilakis, "Optimal distributed generation placement under uncertainties based on point estimate method embedded genetic algorithm," *IET Generation, Transmission, Distribution*, vol. 8, no. 3, pp. 389–400, Mar. 2014.

[32] Y. Cao, Y. Tan, C. Li, and C. Rehtanz, "Chance-constrained optimization-based unbalanced optimal power flow for radial distribution networks," *IEEE Trans. on Power Delivery*, vol. 28, no. 3, pp. 1855–1864, July 2013.

[33] M. Baran and F. Wu, "Network reconfiguration in distribution systems for loss reduction and load balancing," *IEEE Trans. on Power Delivery*, vol. 4, no. 2, pp. 1401–1407, Apr. 1989.

[34] ——, "Optimal capacitor placement on radial distribution systems," *IEEE Trans. on Power Delivery,*, vol. 4, no. 1, pp. 725–734, Jan. 1989.

[35] K. Turitsyn, P. Sulc, S. Backhaus, and M. Chertkov, "Options for control of reactive power by distributed photovoltaic generators." *Proceedings of the IEEE*, vol. 99, no. 6, pp. 1063–1073, June 2011.

[36] M. Farivar and S. Low, "Branch flow model: Relaxations and convexification ;part i," *IEEE Trans. on Power Systems*, vol. 28, no. 3, pp. 2554–2564, Aug. 2013.

[37] D. Taggart, K. Hao, R. Jenkins, and R. VanHatten, "Power factor control for grid-tied photovoltaic solar farms," in *Proc. of 14th Annual Western Power Delivery Automation Conference*, Spokane, WA, Mar. 2012.

[38] W. B. Dan Ton, "Summary report on the doe high-tech inverter workshop," Sandia National Laboratories, Tech. Rep., 2005.

[39] D. L. Evans and L. M. Leemis, "Algorithms for computing the distributions of sums of discrete random variables," *Mathematical and Computer Modelling*, vol. 40, no. 13, pp. 1429–1452, 2004.

[40] A. Prekopa, *Stochastic Programming*. Springer Netherlands, 1995.

[41] K. Ng, C. Moo, Y. Chen, and Y. Hsieh, "Enhanced coulomb counting method for estimating state-of-charge and state-of-health of lithium-ion batteries," *Applied Energy*, vol. 86, no. 9, pp. 1506 – 1511, 2009.

[42] R. Walawalkar, J. Apt, and R. Mancini, "Economics of electric energy storage for energy arbitrage and regulation in New York," *Elsevier;Energy Policy*, vol. 35, no. 4, pp. 2558–2568, Apr. 2007.

[43] H. Akhavan-Hejazi, B. Asghari, and R. Sharma, "A joint bidding and operation strategy for battery storage in multi-temporal energy markets," in *Proc. of IEEE PES Innovative Smart Grid Technologies Conference*, Washington, DC, Feb. 2015.

[44] H. Mohsenian-Rad and A. Leon-Garcia, "Optimal residential load control with price prediction in real-time electricity pricing environments," *IEEE Trans. on Smart Grid*, vol. 1, no. 2, pp. 120–133, Sept. 2010.

[45] http://www.ee.ucr.edu/ ˜ hamed/NPCCData.zip.

[46] "https://dataport.pecanstreet.org/."

[47] "http://ewh.ieee.org/soc/pes/dsacom/testfeeders/index.html."

[48] "https://hvdc.ca/pscad."

[49] "https://www.llnl.gov/."

[50] "http://en.winston-battery.com/index.php/products/power-battery."

[51] B. Jansen, J. D. Jong, C. Roos, and T. Terlaky, "Sensitivity analysis in linear programming: just be careful!" *European Journal of Operational Research*, vol. 101, no. 1, pp. 15–28, 1997.

[52] A. Nemirovski and A. Shapiro, "Convex approximations of chance constrained programs," *SIAM Journal on Optimization*, vol. 17, no. 4, pp. 969–996, 2007.

[53] M. El-Hawary and G. Mbamalu, "Stochastic optimal load flow using a combined quasi-newton and conjugate gradient technique," *Electrical Power and Energy Systems*, vol. 11, no. 2, pp. 85 – 93, Apr. 1989.

[54] M. Brucoli, M. La-Scala, F. Torelli, and M. Trovato, "A new decomposition method for optimal operation of transmission/generation and subtransmission/distribution systems," *International Journal of Electrical Power and Energy Systems*, vol. 15, no. 5, pp. 273 – 282, 1993.

[55] S. Jovanovic and B. Babic, "Decoupled and decomposed power flow solution method," *International Journal of Electrical Power and Energy Systems*, vol. 9, no. 2, pp. 117 – 121, Apr. 1987.

[56] N. Li, L. Gan, L. Chen, and S. Low, "An optimization-based demand response in radial distribution networks," in *Proc. of IEEE Globecom Workshops*, Anaheim, CA, Dec 2012.

[57] *Techno-economical and life expectancy modeling of battery energy storage systems*, June 2011.

[58] D. Zafirakis, K. Chalvatzis, G. Baiocchi, and G. Daskalakis, "Modeling of financial incentives for investments in energy storage systems that promote the large-scale integration of wind energy," *Applied Energy*, vol. 105, pp. 138 – 154, 2013.

[59] A. Leon-Garcia, *Probability, Statistics, and Random Processes for Electrical Engineering*, 3rd ed. Prentice Hall, 2008.

Hossein Akhavan-Hejazi (S'12) received the M.Sc. degree in electrical engineering from Amirkabir University of Technology, Tehran, Iran, in 2011 and the Ph.D. degree in electrical engineering from the University of California, Riverside, USA, in 2016. His research interests include optimization and stochastic analysis in electric power systems, power system operations and market analysis, operation management and modeling of energy storage systems, and big data applications in power systems.

Hamed Mohsenian-Rad (S'04-M'09-SM'14) received the Ph.D. degree in electrical and computer engineering from the University of British Columbia Vancouver, BC, Canada, in 2008. He is currently an Associate Professor of electrical engineering at the University of California, Riverside, CA, USA. His research interests include modeling, analysis, and optimization of power systems and smart grids with focus on energy storage, renewable power generation, demand response, cyber-physical security, and large-scale power data analysis. He received the National Science Foundation CAREER Award 2012, the Best Paper Award from the IEEE Power and Energy Society General Meeting 2013, and the Best Paper Award from the IEEE International Conference on Smart Grid Communications 2012. He serves as an Editor for the IEEE TRANSACTIONS ON SMART GRID and the IEEE COMMUNICATIONS LETTERS.